OIL MONITORING WITH AN OPTICALLY STIMULATED CONTACT POTENTIAL DIFFERENCE SENSOR

A Thesis
Presented to
The Academic Faculty

By

Lisa Marie Ellis

In Partial Fulfillment
of the Requirements for the Degree
Master's of Science in Mechanical Engineering

Georgia Institute of Technology
July 2004

OIL MONITORING WITH AN OPTICALLY STIMULATED CONTACT POTENTIAL DIFFERENCE SENSOR

Approved by:

Steven Danyluk, Ph.D., Chair

Jiri Janata, Ph.D.

Shreyes Melkote, Ph.D.

July 6, 2004

DEDICATION

To my parents

who are my best friends

and biggest supporters.

ACKNOWLEDGEMENTS

First I would like to say a special thanks to my advisor, Dr. Danyluk. I am truly appreciative of your guidance and support through out my graduate career.

Thank you, Dr. Janata and Dr. Melkote for your time and effort in serving on my thesis committee. I would also like to take this opportunity to thank other members of the Georgia Tech community. I would like to thank Dr. Zharin for your input and efforts in designing new probes for me to try, Brandon Steele and Jeff Hawthorne for helping me with circuit issues, and making the probe utilized in my experimentation, Dr. Art Janata and Dr. Mira Josowicz for your friendship and guidance, Dr. Jinata's students for helping me perform analysis of my silicon and oil samples, Markus Janotta and Manfred Karlowatz for your help with the optical part of my experimentation, Ajay Upadhyaya and Vijay Yelundur for their insight and for preparing my nitride coated samples, Daniel Osorno for your friendship, help, and positive attitude, Frank Mess for your advise, insight and friendship, Siarhei Tsiareshka for your help with code and circuit issues, and the rest of my lab mates for their friendship, and support. I appreciate all of your help.

I would also like to thank you Mom and Dad for always being there, your support is what helped me make it through this endeavor. And most importantly, thank you God for blessing me with such wonderful people in my life, and for being my guide.

Finally, thank you Peter Schmidt from the Office of Naval Research for funding this work.

TABLE OF CONTENTS

LIST OF TABLES

LIST OF FIGURES

SUMMARY

This thesis utilized the concept of an optically stimulated Contact Potential Difference (osCPD) sensor to monitor oil properties. The osCPD technique is a variant of the contact potential difference (CPD) method used to obtain surface properties of materials. The technique uses modulated light to stimulate electron charge carriers in silicon coated with a layer of oil. Demonstration of this oil monitoring design was done by placing different oil samples on the silicon surface and monitoring the corresponding electrical signal with the osCPD sensor.

Experiments showed that the osCPD sensor produced an electrical signal that was related to the amount of time an oil sample was aged in an engine (or mileage). Further, a linear relationship was found between the relative conductivity of these oils and the osCPD signal as:

$$Vpp \approx 10\,(1\text{-}K') \qquad \textbf{(1)}$$

where Vpp is the osCPD peak-to-peak voltage and K' is the relative oil conductivity. It is theorized that this osCPD signal is dependant on the charge transfer at the silicon and oil interface. Investigation of this interaction was carried out. Experiments showed that adding a silicon nitride passivation layer on the silicon surface eliminated the change in osCPD signal with oil properties. A model of this charge interaction was developed.

CHAPTER 1

INTRODUCTION

This thesis addresses the use of a non-vibrating Kelvin probe along with a pulsed light source to monitor an oil film that was placed on a single crystal silicon surface. The pulsed light was shown on the bottom surface of the silicon and created charge carriers which diffuse through the silicon to the surface where the oil had been placed. The probe is placed directly above this oil coated surface and separated from the oil film by a mica spacer. The resulting sensor signal is believed to be dependant on the charge interaction between the oil and silicon surface.

Kelvin probe sensors measure contact potential difference (CPD) which is related to the change in surface potential or work function of the surface of interest. The work function is the minimum energy required to remove an electron from the Fermi energy level to just outside the conductor surface. To perform CPD measurements, Kelvin probes generally use relative motion, either vibration or translation of one surface relative to the other (i.e. probe surface relative to surface of interest). The proposed non-vibrating probe or optically stimulated Contact Potential Difference (osCPD) sensor uses pulsed light, instead of relative motion, to perform CPD measurements.

The objective of this thesis is to show that the osCPD sensor can monitor oil properties, and that the resulting signal is dependant on the charge interaction between the oil and silicon surface. To validate the first objective, the sensor signal was collected for oil samples that had been aged in an engine. The resulting osCPD signal was then compared to the conductivity of these engine oil samples (as conductivity is a measure of

oil degradation). The mechanism for the signal was investigated by passivating the silicon surface with a nitride layer.

CHAPTER 2

BACKGROUND

Surface Potential of Conducting Materials

The work function or surface potential, Φ, of a conductor is the energy required to remove an electron from the Fermi energy level to just outside the surface or the vacuum reference level. Figure 1 illustrates the electronic band structure of a conductor in a vacuum at absolute zero. The potential energy just outside the surface is defined as zero and the work function,Φ, is the lowest energy required to remove an electron from the bulk material to just outside the surface. It is the difference in work function between two materials that defines contact potential difference.

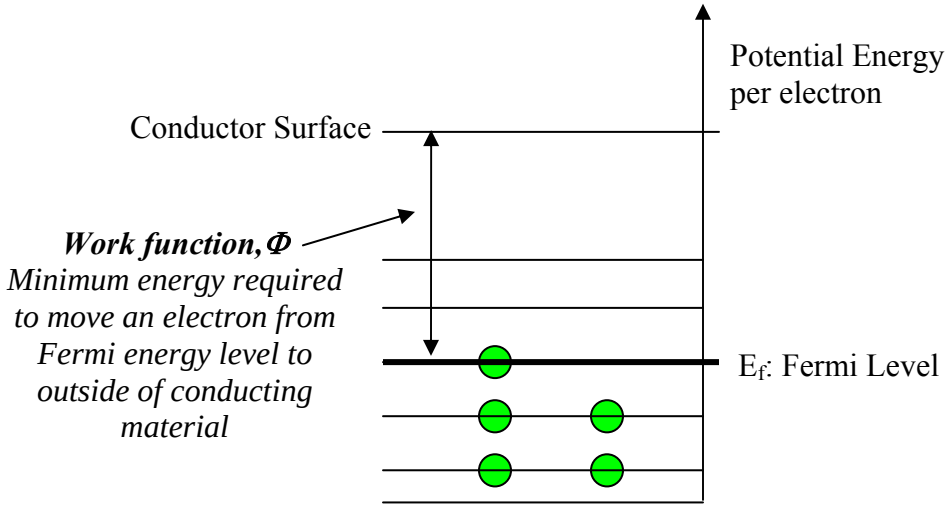

Figure 1. Electronic Band Diagram of a Conductor in a vacuum at absolute zero.[1]

Definition of Contact Potential Difference

Contact potential difference (CPD) is the difference in work function between two conducting materials. Figure 2 shows a schematic diagram of the band structure of two conducting materials not in contact. Each conductor has an individual Fermi energy, and the potential energy of both surfaces is taken as zero just outside the surface. When these two conductors are electrically connected, as shown in Figure 3, electrons will tend to flow from the material with higher potential energy (Conductor 1) to the one with lower potential energy (Conductor 2). The charge flow will appear instantaneous and cease when the Fermi energies equilibrate. This transfer of electrical charge will result in a net negative charge in one material balanced by a positive charge in the other. With the Fermi energy being chosen as the new reference of potential, the voltage between these two can be related to the work function of each material (Φ_1 and Φ_2) by:

$$\Delta V = \frac{\Phi_2 - \Phi_1}{|e|} \qquad (2)$$

where e is the charge of an electron and ΔV, or V_{CPD}, is defined as the contact potential difference of the two conductors.

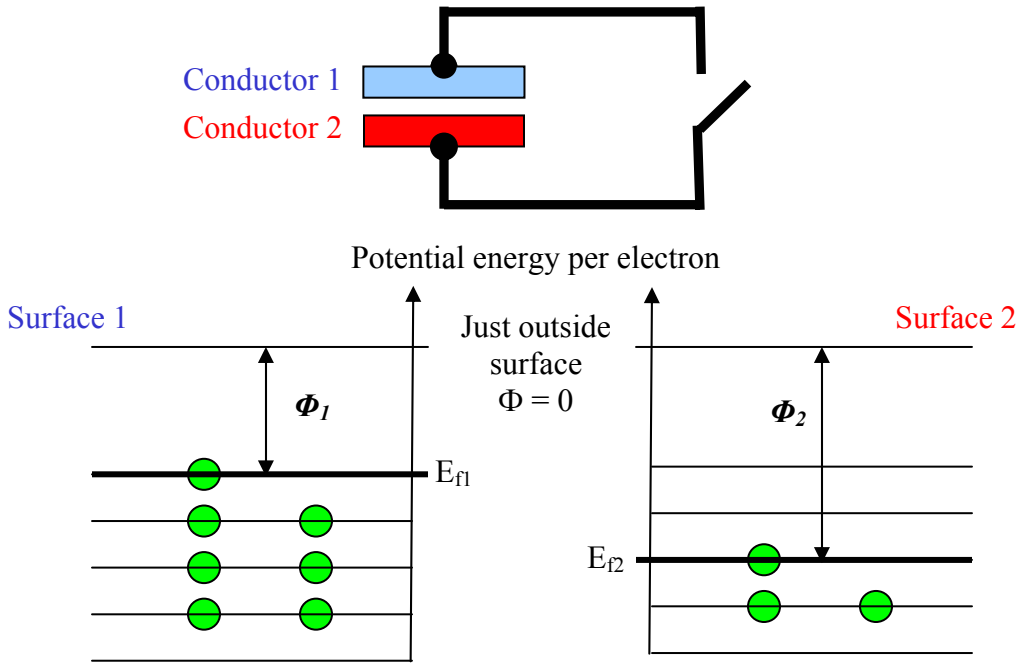

Figure 2. Energy level diagram of the work function of two metals in close proximity with no electrical contact.[1]

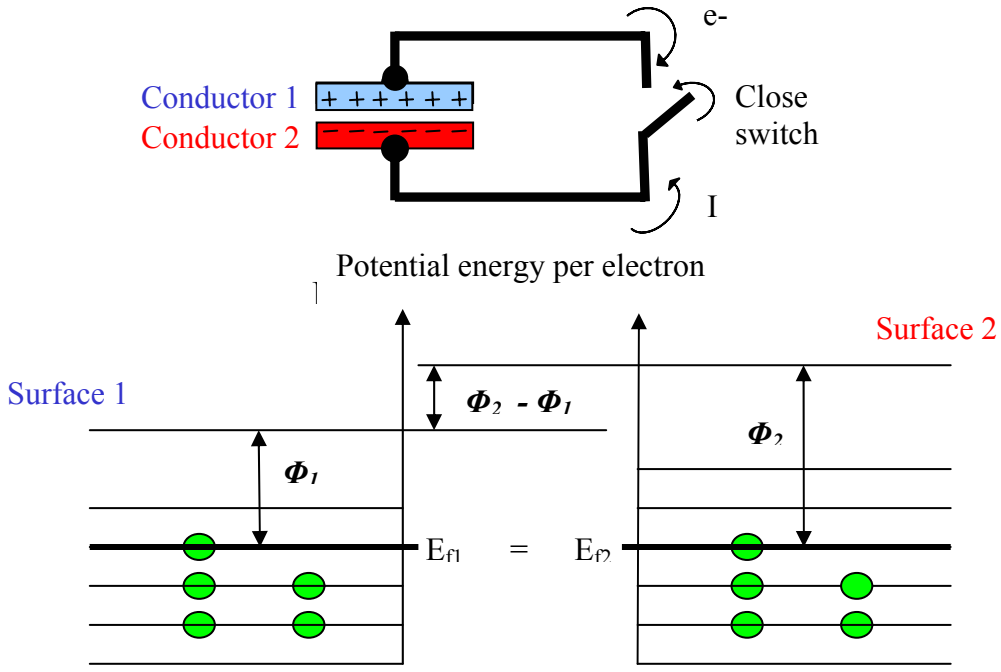

Figure 3. Energy level diagram of the work function of two metals in close proximity with electrical contact.

The charge on the surfaces and contact potential are related by:

$$q = C(\Phi_2 - \Phi_1) = CV_{CPD} \quad \textbf{(3)}$$

where C is the constant of proportionality, the capacitance that develops between the surfaces. A simplified model is to assume that the surfaces are flat and comprise a parallel plate capacitor. Thus the charge on the surfaces, q, is related to capacitance, C, and contact potential difference (Vcpd) as:

$$q = CV_{CPD}$$

where the capacitance for a parallel plate geometry is given by:

$$C = \frac{\varepsilon_r \varepsilon_o A}{d} \quad \textbf{(4)}$$

where ε_r is the relative dielectric constant, ε_o is the permittivity of free space, A is the area of surfaces, and d is the spacing between the two plates.

Any relative motion of the two surfaces or a change surface characteristics with time will result in a current that would flow between these two surfaces:

$$i = \frac{dQ}{dt} = \frac{d(CV_{CPD})}{dt} = V_{CPD}\frac{dC}{dt} + C\frac{dV_{CPD}}{dt} \quad \textbf{(5)}$$

Kelvin Probe

The Kelvin probe is a capacitor sensor that measures the contact potential difference (CPD) between two dissimilar conducting materials. In 1898, Lord Kelvin found this potential difference was visible on a gold leaf electroscope when he electrically connected two dissimilar metals.[2] This response was momentary and difficult to quantify, but in 1932 the probe was modified by Zisman such that one electrode

vibrated with respect to the other.[3] He proposed that the change in spacing between the two electrodes or time varying capacitance created a current proportional to the CPD between the two metals. Thus if the work function of the vibrating electrode was known, the work function of the other metal could be determined. This probe is typically used to study the work function and surface potentials of metals and dielectrics.

Non-Vibrating Contact Potential Difference Sensor

An alternate way to obtain CPD measurements proposed by Danyluk and Zharin is using translation.[4] Relative motion of the surface will result in electrical signals if there is a geometrical or chemical change occurring. The signal will reflect time varying changes in the CPD of the surface, rather than the absolute CPD as in the case of the Kelvin probe.

Optically-Stimulated Contact Potential Difference Sensor

This thesis proposes a new technique based on contact potential difference measurements. Instead of using a vibrating probe or a translating surface, the time varying current required to generate a signal is created by a chopped light source.

In this technique, chopped light illuminates a silicon substrate at some appropriate wavelength with the incident photon energies sufficient (greater than band gap of silicon) to excite electrons from the valence band to the conduction band. In the presence of an electric field (created by the difference in surface potentials between the semiconductor and probe surface), these photoexcited electrons diffuse through the silicon.

As shown in Figure 4, the chopped light is directed at surface 1, and the electrons diffuse towards surface 2 due to the electric field. Not all electrons reach surface 2, i.e. contribute to total charge on it's surface, some are lost to recombination. The time varying change of this charge on surface 2 (or current) is measured by the osCPD probe and can be expressed as:

$$i \approx \text{Jph} - \text{Jo} \qquad \textbf{(6)}$$

where Jph is the photoexcited electrons and Jo is current loss due to electron recombination. [5]

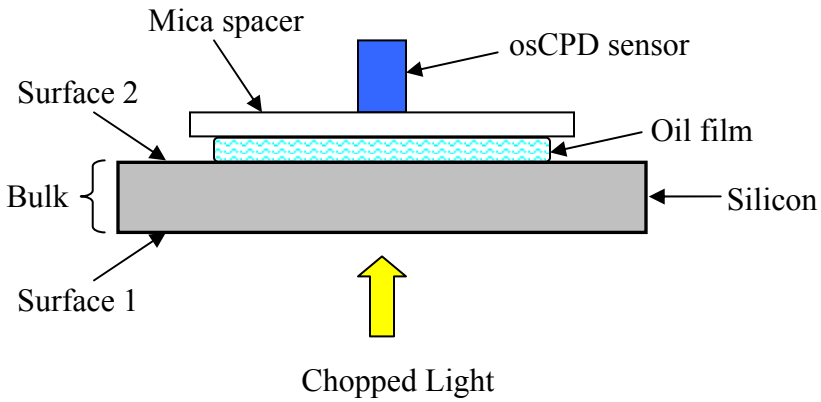

Figure 4. Schematic diagram illustrating the geometry of the osCPD experiment in relation to the oil and silicon substrate.

The electrons recombine at surfaces and in the bulk of the silicon substrate. Thus the recombination current, Jo, can be re-written as follows:

$$\text{Jo} = \text{Js1} + \text{Jbulk} + \text{Js2} \qquad \textbf{(7)}$$

where Js1, Jbulk and Js2 is the recombination at surface 1, in the bulk, and at surface 2 respectively. The recombination current at surface 2, where oil is placed, can further be described by the following equation for semiconductor/liquid junctions:

$$Js2 = q\ k\ n\ [A] \qquad \textbf{(8)}$$

where q is a constant, k is the heterogeneous rate of electron transfer at the junction, n is the concentration of photo-generated electrons at the silicon surface, and [A] is the concentration of acceptor species at the surface.[6-7] After substituting Equations 7 and 8 for the recombination current, the osCPD current, Equation 6, or the total measured charge on surface 2 becomes:

$$i = Jph - (Js1 + Jbulk + q\ k\ n\ [A]) \qquad \textbf{(9)}$$

This signal is converted to a voltage, and the resulting osCPD measured voltage becomes:

$$Vpp = G\ (Jph - Js1 - Jbulk\ - q\ k\ n\ [A]) \qquad \textbf{(10)}$$

where G is the effective resistance.

Effect of Passivation of Silicon Surface on Recombination

Depositing a nitride layer onto the silicon surface with plasma enhanced chemical vapor deposition (PECVD) passivates the surface.[8] Using this process on the silicon surface lowers the surface recombination velocity, k, by at least two orders of magnitude as compared to an uncoated, bare silicon wafer.[9] Along with this, passivating the surface separates the charge interaction between the silicon and liquid junction.

CHAPTER 3

EXPERIMENTAL SETUP

This chapter describes the osCPD sensor system. First a review will be given of the overall experimental design, then a detailed description of the system components.

Overall System Design

A schematic diagram of the osCPD system is shown in Figure 5. The system functions as follows: using a fiber optic light pipe, light from a 50W halogen source is directed through a 5 mm diameter hole in the grounded copper stage to the underside of the silicon substrate. A 450 nm band pass filter is placed on top of this light pipe to filter the light to the selected wavelength range. The light is then modulated using the 10 blade optical chopper, the frequency of which is controlled using the MC1000 optical chopper controller. The controller sends a reference signal to the data acquisition system so that the osCPD signal can be triggered at the selected chopper frequency.

A drop of oil is placed on the silicon substrate and then covered by a mica spacer to keep the sensor from being contaminated by different oil samples. After placing this sample on the stage, the vertical positioning system is used to lower the probe so that it compresses into the mica cover. The sensor signal is then sent to the data acquisition card.

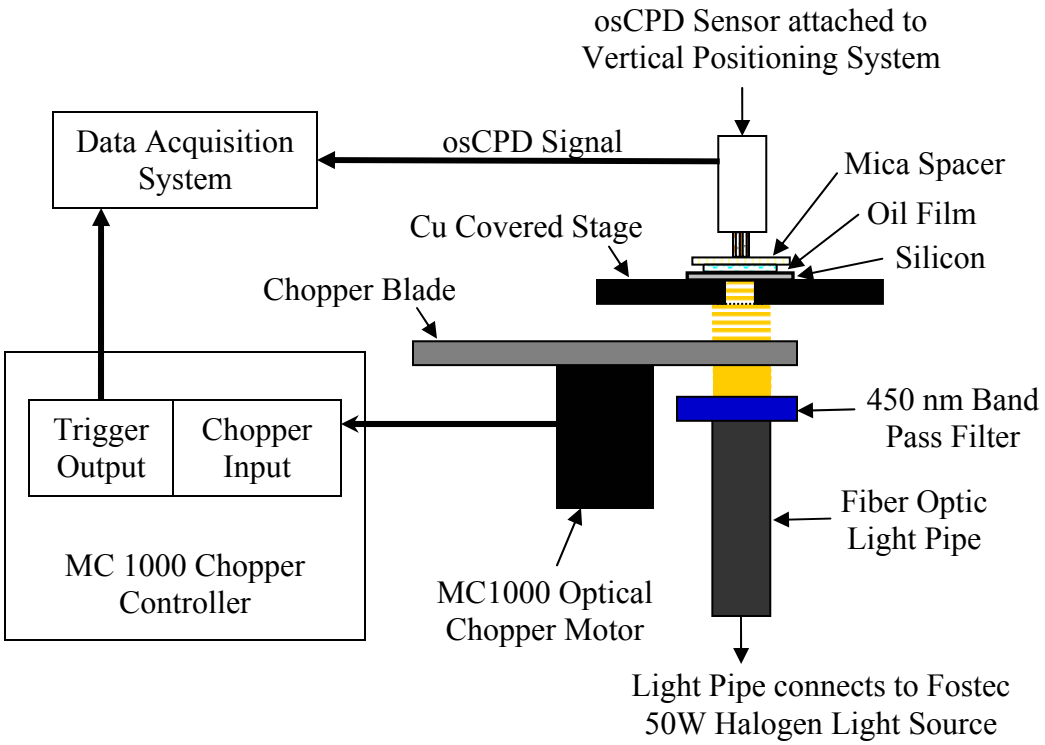

Figure 5. Schematic diagram of osCPD oil monitoring system.

System Components

A photograph of this set-up with major system components highlighted is in Figure 6.

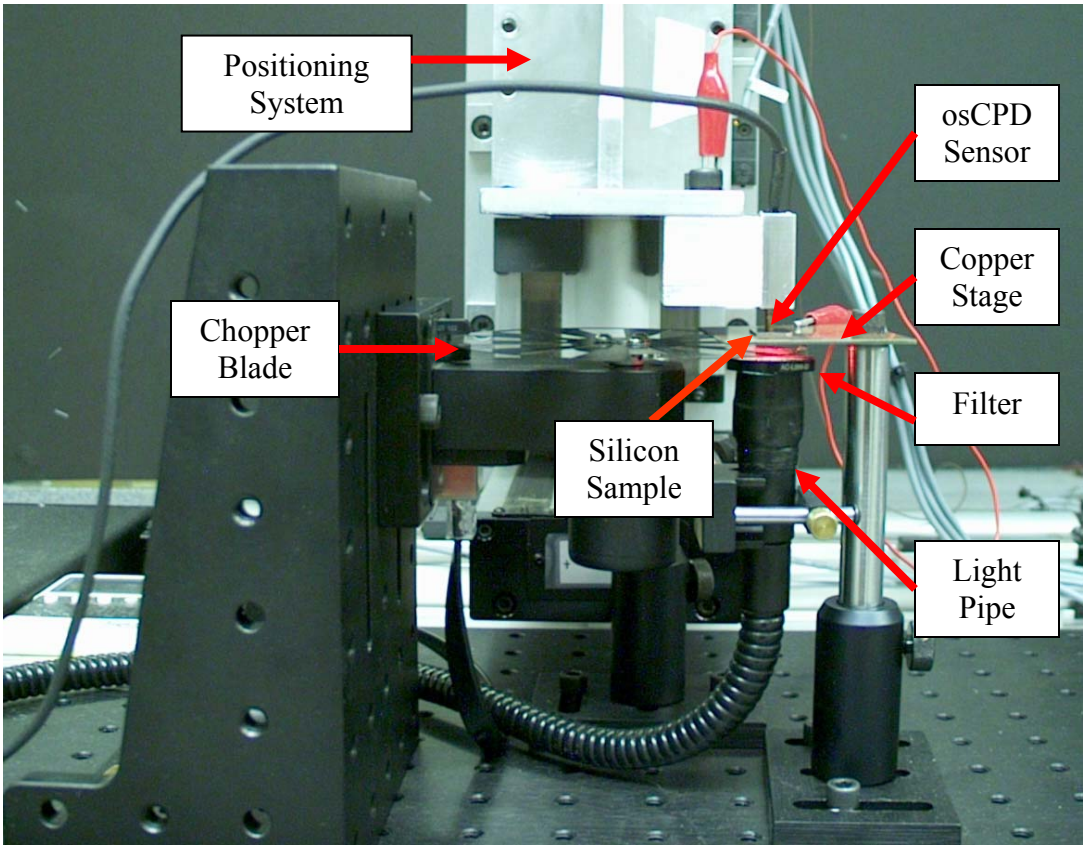

Figure 6. Photograph of experimental set-up with major system components highlighted.

osCPD Sensor

Figure 7 illustrates the basic design of the probe which consists of 0.5 mm copper wire surrounded by a metal sheath. The metal sheath, 3 mm in diameter and 0.5 mm thick, is separated from the central copper conductor by a polyethylene sleeve. This is a typical probe tip configuration utilized by the CPD research group at the Georgia Institute of Technology.[10-11] The shield surrounding the copper wire reduces fringe electrical fields. Research is currently being done on the effect of the shield in reducing electrical fields. This probe tip is connected to the sensor circuitry as shown in Figure 8. At the center of the electronics is the A250F Amtec charge sensitive preamplifier. The circuit is

a typical charge sensing circuit, and a similar diagram can be found in the preamplifier data sheet.[12]

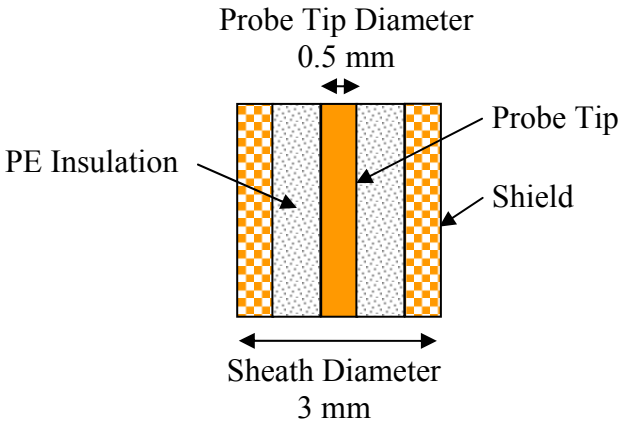

Figure 7. A schematic diagram of the cross section of the osCPD sensor.

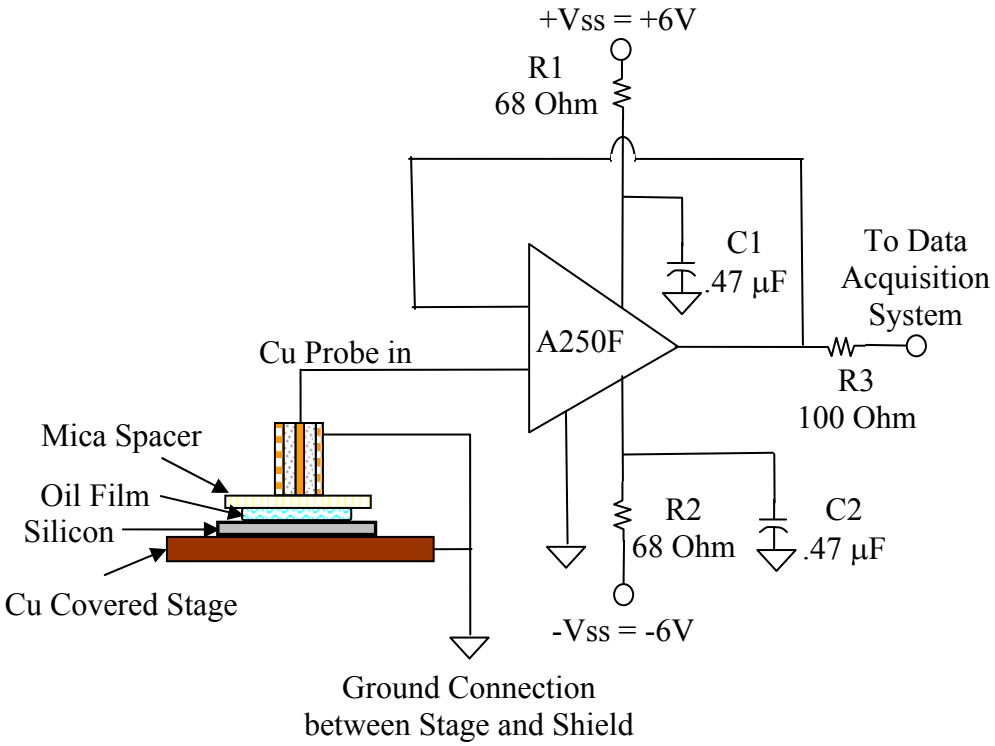

Figure 8. Circuit diagram of osCPD sensor system.

Figure 9 shows a schematic diagram of an expected osCPD signal. This figure shows the relationship between the voltage signal and light intensity. A positive spike is generated by turning on the light, and is followed by the negative spike as the light is blocked by the mechanical chopper.

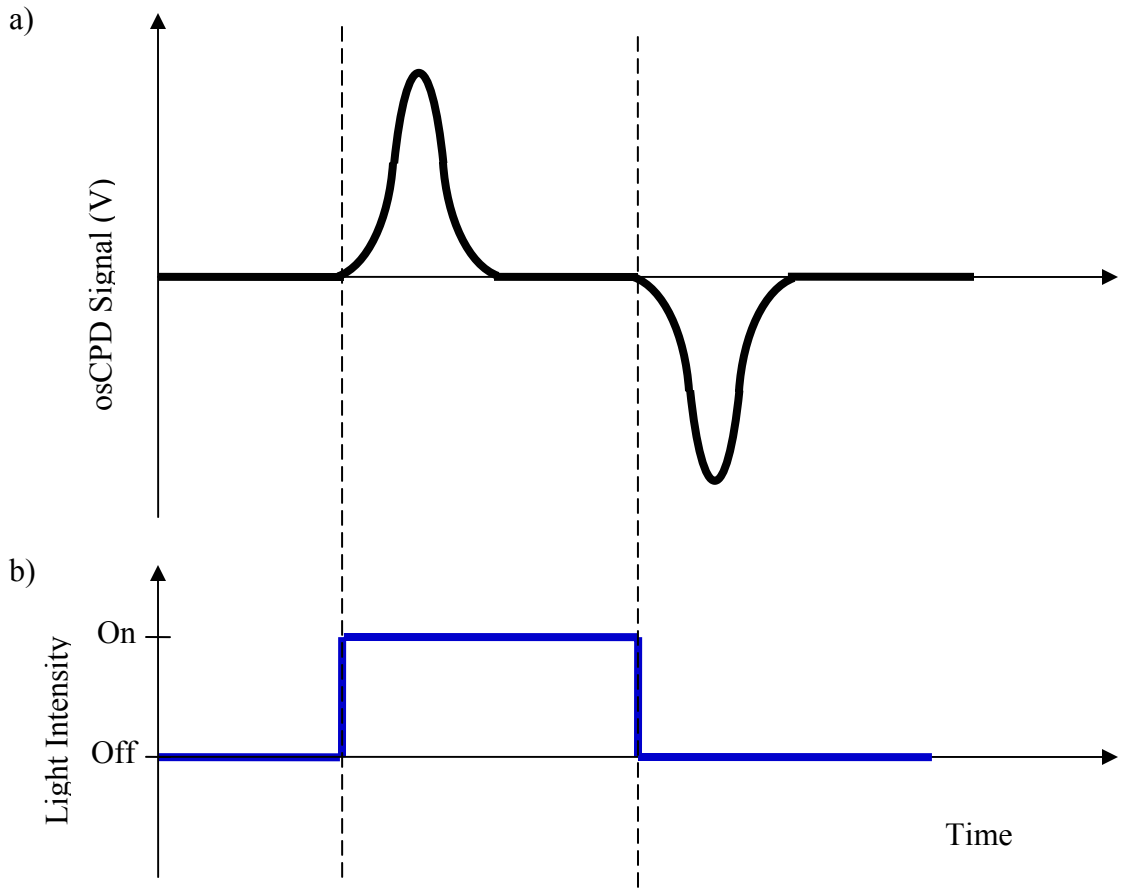

Figure 9. Schematic diagram of the expected osCPD signal in relation to incident light on the silicon substrate. 9a represents the expected osCPD signal over time. 9b represents the transition of light on and off over time.

Optical Components

The optical components include the fiber optic light, the Fostec 50W Halogen light source, the 450 nm band pass filter, and the MC1000 optical chopper. The Fostec 50W Halogen source is set to a maximum. The 450 nm band pass filter transmits wavelengths ranging from 440 nm to 460 nm. This light was selected to ensure that incident photons have sufficient energy (greater than band gap of silicon) to excite electrons from the valence band to the conduction band. Since a wavelength of 450 nm corresponds to an energy of 2.7 electron volts (eV) and the band gap of the silicon used is 1.1 eV, then this light source meets the requirements. The Thor Labs MC1000 optical chopper is used to modulate the incident light at the selected frequency of 400 Hz. Table 1 below summarizes the optical component settings.

Table 1. Optical component settings.

Optical Setting Description	Setting level
Fostec Light Source Setting	100 % Intensity
MC 1000 Optical Chopper frequency	400 Hz
450 nm Band Pass filter range	440 to 460 nm

Positioning System

A computer controlled servo motor positioning system was used to provide precise mobility of the osCPD sensor in the vertical direction. With 1 micron accuracy, the servo motor system raises and lowers the sensor to two selected heights. The first predefined height is set so that the probe sensor is lowered to the mica sample surface. The second height is 2 cm above the substrate surface so that the silicon sample can be removed between tests.

Data Acquisition System

The data acquisition system consists of hardware and software. The NiDAQ 68 pin shielded connector block and the 12 bit data acquisition card serve as the main system hardware. The resolution of the data acquisition card with a +/- 5 volt nominal output range is 0.557 mV. This card provides voltage to the amplifier in the osCPD sensor and collects the signal from the osCPD sensor and chopper controller.

The data acquisition system is set to sample at 200 kHz and record 500 data points after receiving a trigger input from the chopper (chopper blade passes underneath the sensor on the chopper). With the chopper rotating at 400 Hz, then collecting 500 data points corresponds to one period between the start of one chopper blade to the start of the next one. Thus at each trigger input, one period of light shining on and off the silicon substrate is recorded. From these 500 data points, the data acquisition system subtracts the maximum minus the minimum osCPD signal to get the peak-to-peak voltage. The peak-to-peak signal is recorded for 5 seconds and then averaged. A summary of the data acquisition settings are shown in Table 2 below.

Table 2. Data acquisition settings.

Data Acquisition Settings	Value
Sampling rate	200 kHz
Scan length	500 data points
Scan time	5 seconds

The software utilized includes: Motion Control, Data Acquisition, and the Quad program software. The motion control system raises and lowers the probe to the heights specified in the code. The user interface and code are shown in Appendix A. The data

acquisition software, shown in Appendix B, collects the osCPD signal, and is triggered by the optical chopper. Finally, the quad program controls both the motion and data acquisition software (interface and code in Appendix C). At a push of the button on the Quad program, the probe is lowered, the osCPD signal is collected for the desired amount of time and then the probe is raised back up.

Experiment Sample Components

The experimental sample consists of three components: silicon, oil and mica. The silicon samples were diced from 6 inch double side polished boron doped p-type, (100) silicon wafers with 10-20 Ω/cm resistivity and a thickness of 600 microns. The wafer was diced into rectangular shaped samples with dimensions 10 by 15 mm. The nitride coated silicon samples were made using Plasma Enhanced Chemical Vapor Deposition (PECVD). Several of the diced silicon samples were coated using the PECVD process to produce a nitride layer that was approximately 750 angstroms thick.

The oil samples are from a common engine lubricant oil, Pennzoil 10W-30 viscosity grade, used in automobile engines. The oil was aged and collected from a passenger car which consistently used Pennzoil 10W-30.[13] Oil samples were removed from the car at 235, 4080, 8376 miles. Other analysis, including gas chromatography and mass spectrography, has been published using these oil samples.[13-14]

The mica spacers, used to prevent contamination of the osCPD probe, were made by splitting a mica sheet to a thickness of approximately 0.02 mm and then cutting the sheet into 10 by 15 cm rectangular shaped samples.

CHAPTER 4

EXPERIMENTAL PROCEDURE

The following describes the overall osCPD measurement technique, the process used to prepare samples, and a review of the experiments performed.

Collection of osCPD signal

Figure 10 shows the flow chart for experimental procedure for taking osCPD measurements:

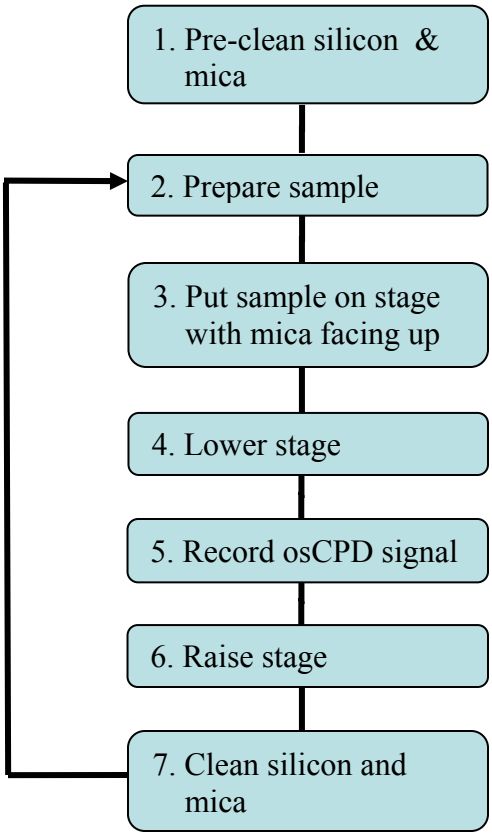

Figure 10. Flow chart of the experimental procedure for collecting osCPD signals.

Sample Preparation Technique

As shown in Figure 10, the measurement process starts with pre-cleaning. The silicon sample is first cleaned with Petroleum Ether then dipped in a Hydrofluoric Acid bath (50% concentration) for 1-2 minutes or until the surface appeared hydrophobic. A hydrophobic surface indicates that the oxide layer has been removed from the surface.[15] After the acid bath, the sample is rinsed in de-ionized water for one minute. The mica spacer is rinsed twice with Petroleum Ether and dried with a Chem-wipe.

A drop of oil is then placed on the cleaned silicon sample using a pipette. After the oil droplet is formed, the mica spacer is placed on top of it. A new pipette is used for each oil sample.

After the osCPD measurement, the following cleaning process is performed. The silicon and mica spacer are rinsed twice with Petroleum Ether and dried with a Chem-wipe. The sample is then prepared for the next oil measurement, and the process is repeated. The following set of experiments use this procedure to collect osCPD measurements.

Light Intensity and Frequency Response Experiments

The osCPD peak-to-peak voltage was recorded for a silicon sample with new oil on the silicon surface as the light intensity control knob was varied. The relation between light intensity setting and light intensity output is shown in Figure 11 below. This test was performed to show the signal dependence on increasing light intensity or the amount of charge carriers input into the system.

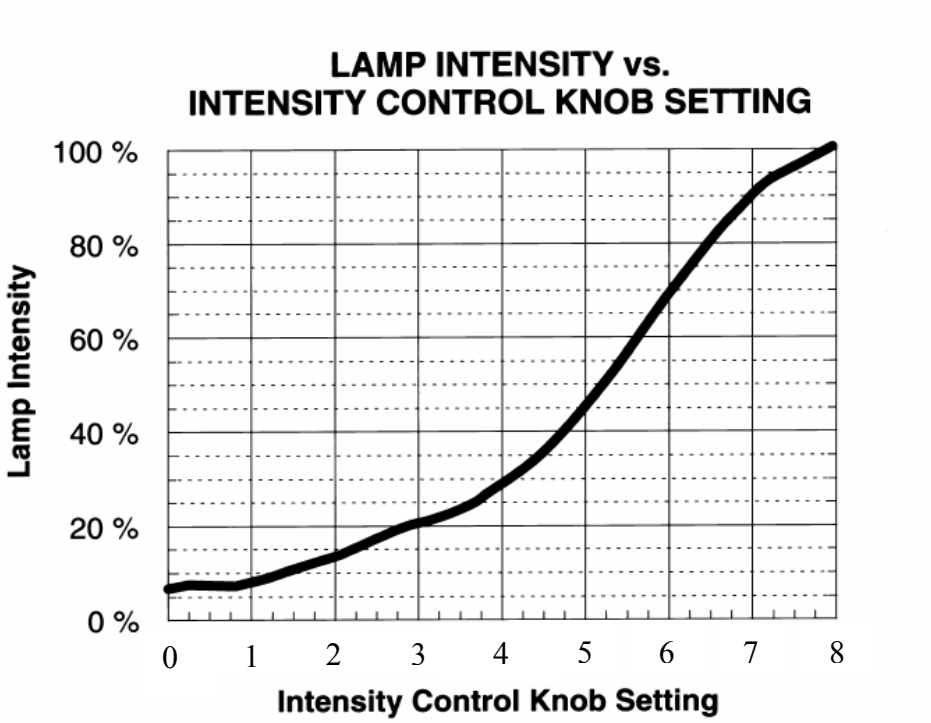

Figure 11. 50W Light source lamp output intensity versus intensity control knob setting.[16]

The frequency of the chopper was also varied to show that the output signal was dependant on the frequency of light incident on the silicon substrate. The osCPD signal was collected at the following frequencies: 50, 100, 200, 400, 600 and 800 Hz for a silicon sample coated with new oil.

Oil Sample Experiments

The osCPD signals of the four different oil samples along with a baseline measurement with no oil were collected in a randomized order (shown in Appendix E) using the procedure shown in Figure 10. For each of these 5 variations (4 different oils, and no oil), 5 repeat trials were performed. The same wafer and spacer were used

throughout the test. This test was performed twice to evaluate the repeatability. The randomization order was changed for the second test and is shown in Appendix E as well. A summary of this oil sample experiment is provided in Table 3 below.

Table 3. Scope of oil sample experiment.

Description	Repetition Amount
Total number of repeat experiments	2
Number of oil measurement repetitions per sample	5

Nitride Coated Sample Experiments

The oil sample experiment was repeated for silicon samples with nitride coatings in various orientations. A diagram of these set-ups as compared to the standard measurement technique with no nitride film is shown in Figure 12. The first experiment tested the osCPD response to oil age using a silicon sample that had a nitride coating on the bottom surface (Figure 12b). Then the silicon sample was flipped over, and measurements were taken with the nitride layer between the oil and silicon interface (Figure 12c). Finally, the process was repeated for a silicon sample with a nitride coating on both the top and bottom surface (Figure 12d). Five repeat measurements were collected in a randomized order for each oil sample in the above tests.

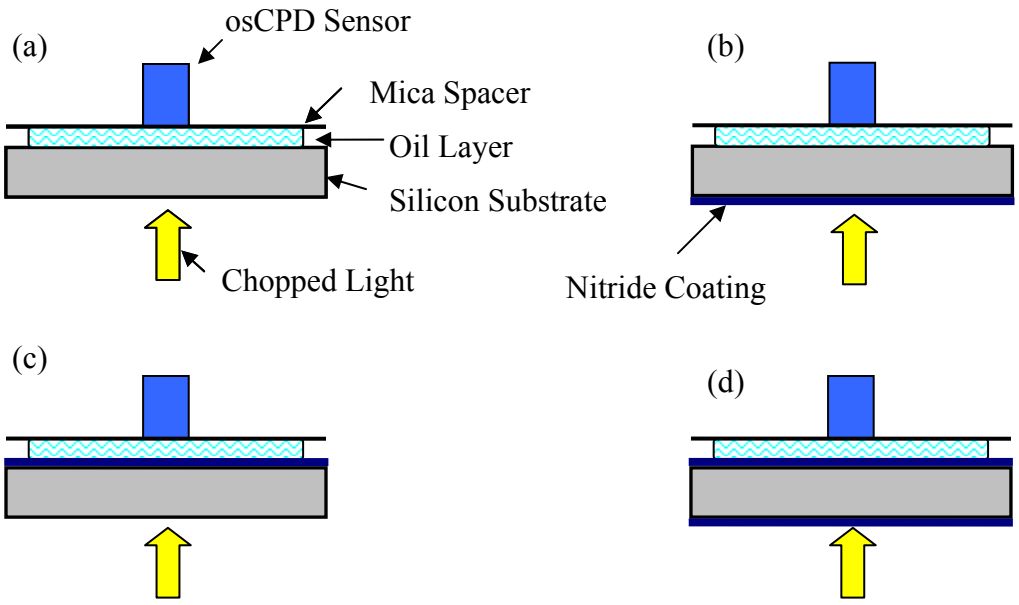

Figure 12. Schematic diagram of the different nitride samples used to evaluate the osCPD response to oil sample mileage. A) is the standard set-up with no nitride coating on the silicon, B) has a coating on the underside, C) has nitride coating on top surface and D) has nitride coating on both surfaces of the silicon.

Conductivity Tests

The conductivity of the engine oils was measured using the Solartron SL1260 Impedance analyzer. A 4 pole conductivity cell was utilized for this measurement. It works by driving a current thru two electrodes and producing a voltage across the other two to determine the conductivity of the sample. The cell was cleaned with Petrol Ether before each measurement. The measurements were taken for one minute for each sample in a randomized order.

CHAPTER 5

RESULTS

This chapter describes the experimental results for testing the ability of the osCPD sensor to detect changes in oil. These results include the variation of the osCPD voltage with light properties, oil sample mileage, nitride coating, and conductivity.

osCPD Signal Dependence on Light Properties

The osCPD response to light intensity and frequency are shown in Figure 13 and Figure 14 respectively. The osCPD peak-to-peak voltage (Vpp) for each light intensity setting represents an average of 2000 peak-to-peak measurements and the error bars are the corresponding 95% confidence interval. The results show a linear relationship between Vpp and light intensity. In the graph showing osCPD signal dependency on frequency, the signal was measured twice at each chopper frequency and a one to one relationship with chopper frequency was found. This in-phase relationship shows that k, the rate of electron transfer is less than one millisecond. Thus, the osCPD signal is linearly related to both light intensity and frequency.

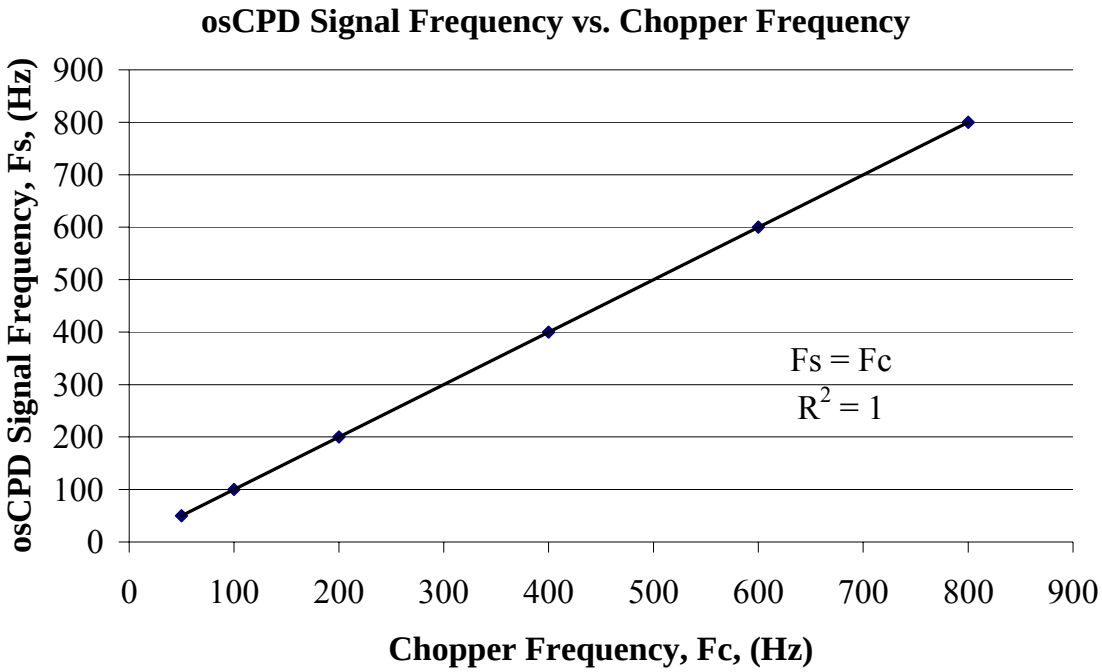

Figure 13. osCPD peak-to-peak voltage (V) of a silicon sample with new oil on the surface versus light intensity (%). There is a linear relationship between Vpp and light intensity.

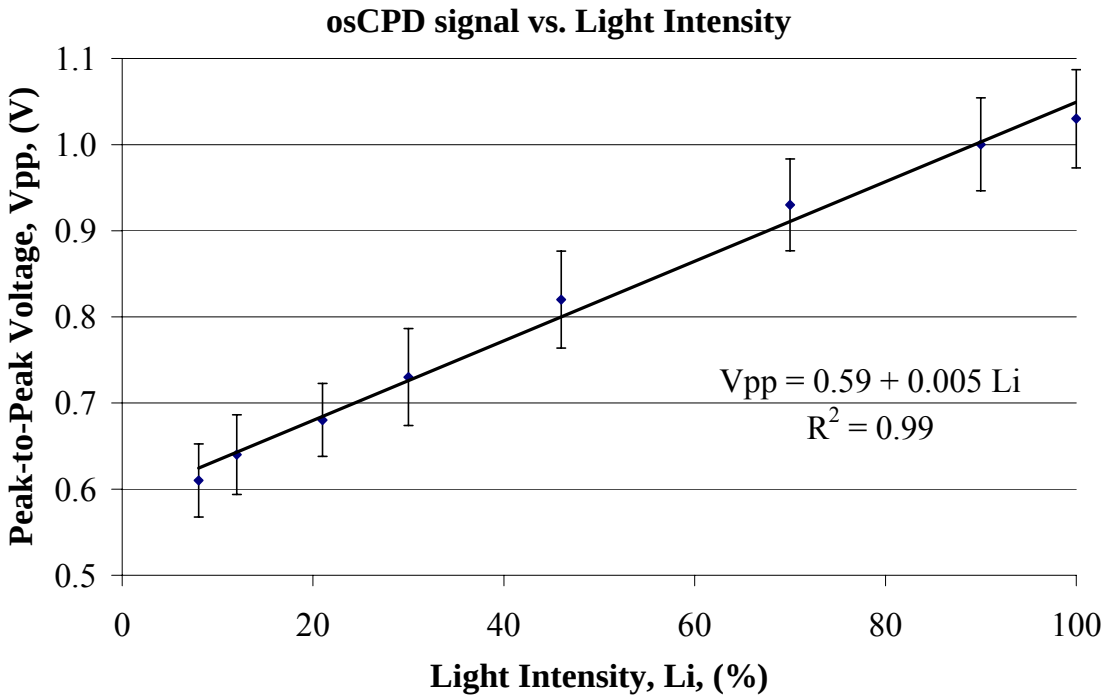

Figure 14. Frequency of osCPD signal (Hz) taken on a silicon sample coated with new oil versus chopper frequency (Hz). There is a perfectly linear relationship between chopper and signal frequency.

Oil Sample Experiments

The results from two trials of experiments measuring the osCPD signal for the 4 oil samples and the baseline measurement with no oil are shown in Figure 15. The peak-to-peak voltage represents an average of five osCPD peak-to-peak measurements, and the error bars represent the 95% confidence interval of this data. This figure shows no change in signal between a freshly prepared silicon surface (no oil) and new oil on the silicon, and a decrease in signal with increasing mileage.

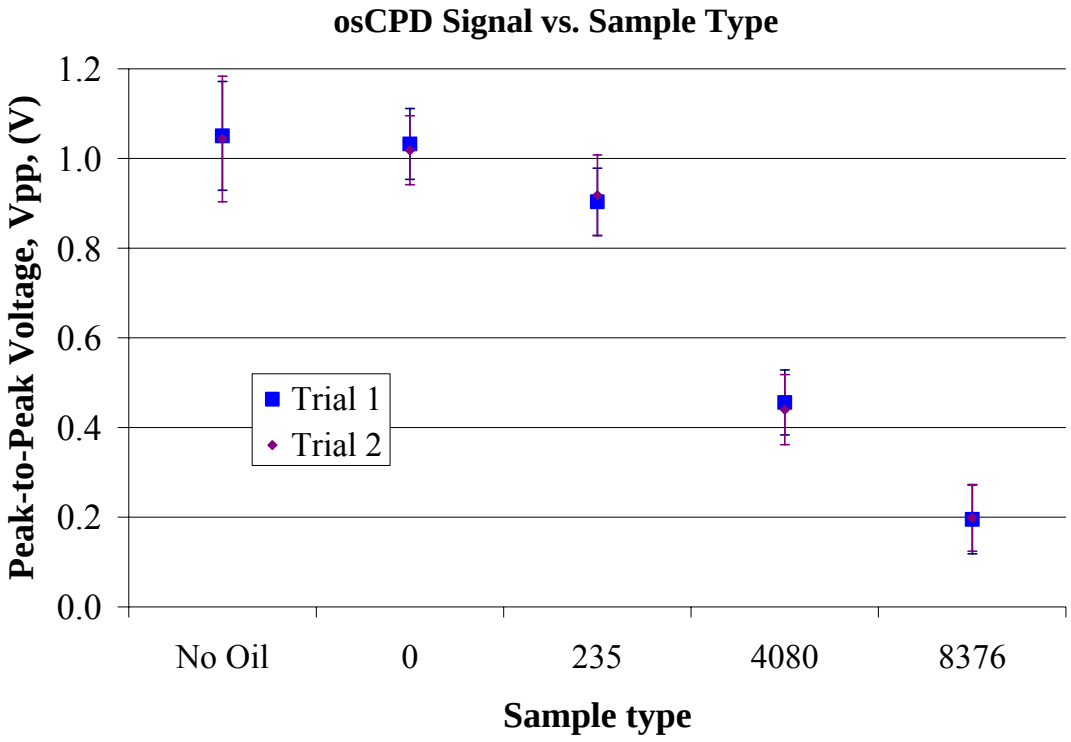

Figure 15. osCPD peak-to-peak voltage (V) for four oil samples and baseline measurement with no oil for two repeat trials using the same silicon substrate.

To better illustrate the osCPD signal response to changes in oil properties, Figure 15 was re-plotted in Figure 16 with the data for no oil removed.

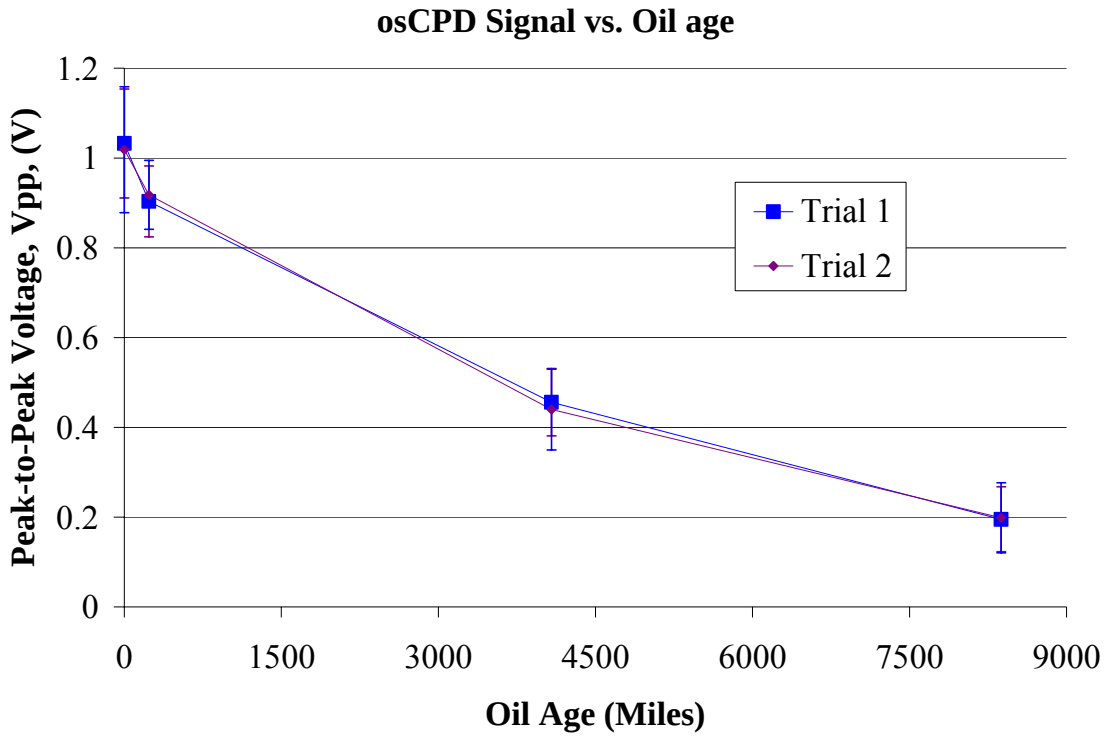

Figure 16. osCPD peak-to-peak voltage (V) versus oil sample age (miles).

The oil sample experiments showing the osCPD peak-to-peak measurements of the different oil samples (Figure 15 & Figure 16) illustrates the ability of the osCPD sensor to detect oil aging or time of use in engine. A two-sample t-test was performed to determine if the osCPD signal was significantly different between these measurements (Minitab output in Appendix D). At the 95% confidence interval, the results confirm that the peak-to-peak voltage for oil samples with mileages 0, 235, 4080 and 8376 miles are

statistically different, but that it can not be shown that there a statistical difference between no and new oil.

The change in osCPD signal with mileage appears to be the same for both trials of experiments, and the variation between the oil samples appears uniform as shown in Figure 15 and Figure 16. This consistency is an indicator of the ability of the cleaning process and experimental procedure to produce repeatable results.

Nitride Coated Sample Experiments

The nitride coating experiments utilize two silicon samples, one silicon sample with a nitride layer on one side, and another silicon substrate with a nitride coating on both sides. For the single sided sample, the test performed evaluates the effect on osCPD peak-to-peak voltage when the aged oil samples are put on the nitride coated sided, and then on the non-coated side. The same effect is evaluated on the double sided nitride coated sample. Figure 17 shows the results from the nitride coating experiments. The peak-to-peak voltage represents an average of 5 peak-to-peak measurements for each data set, and the error bars represent the 95% confidence intervals.

As seen in Figure 17, the osCPD signal decreases with mileage when oil sits on the silicon surface for the single side nitride coated sample, as seen in the previous oil experiments (Figure 15). When oil is placed on the nitride coated side for both the single and double sided nitride coated silicon, there is no longer a decrease in signal with increasing mileage.

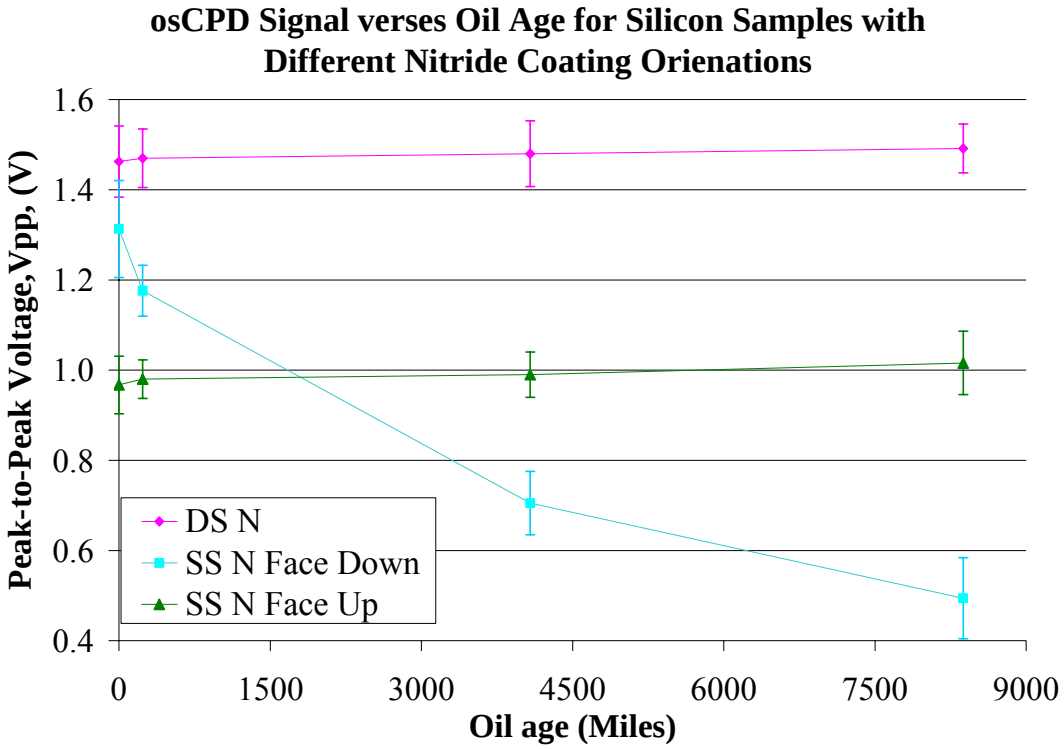

Figure 17. osCPD peak-to-peak voltage (V) versus oil age (miles) for three silicon samples: DS N, SS N Face Down, and SS N Face Up which means double sided nitride coated silicon, single sided nitride coated silicon with the nitride layer facing down, and single sided nitride coated silicon with the nitride layer facing up (oil on nitride layer) respectively.

When the nitride coating is face up, for both the single and double side coated wafers, the measured osCPD value is greater for the double sided sample than that of the single sided piece. To compare the relationship between mileage and osCPD signal for both of these samples, the data was normalized by shifting each average peak-to-peak measurement such that peak-to-peak value of new oil was equal to 1. This normalized data, Figure 18, illustrates that the peak-to-peak voltage appears to slightly increase with mileage for both samples, although statistical analysis performed on this data (shown in Appendix E) shows no significant difference between the oil samples

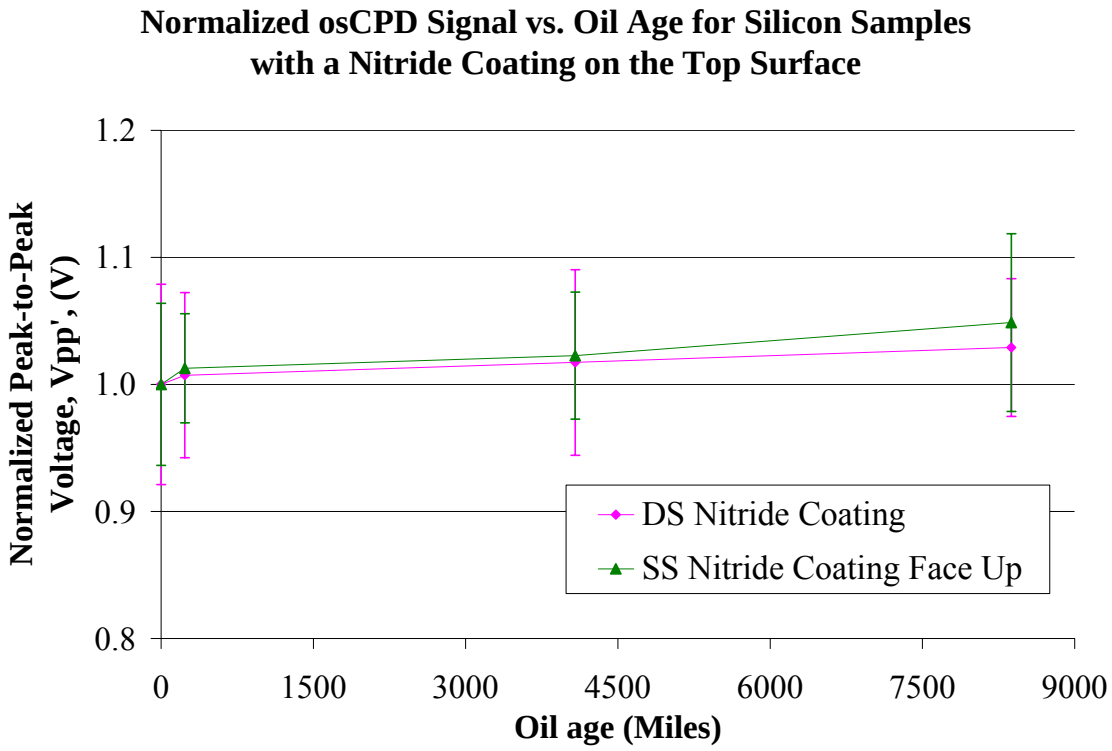

Figure 18. Normalized osCPD peak-to-peak voltage (V) versus oil sample age (miles) for two silicon samples: double sided and single sided nitride coated silicon samples (where the oil is placed on the nitride coated side).

The osCPD response to mileage when oil samples are placed directly on the silicon surface for the single sided and non nitride coated silicon samples is displayed in Figure 19. The data for the non-nitride coated sample came from Trial 1 of Figure 16. The decreasing trend for peak-to-peak voltage as mileage increases appears to be the same for both silicon samples, but the magnitude of the osCPD voltage is approximately 0.3 volts greater for the substrate with the nitride coating.

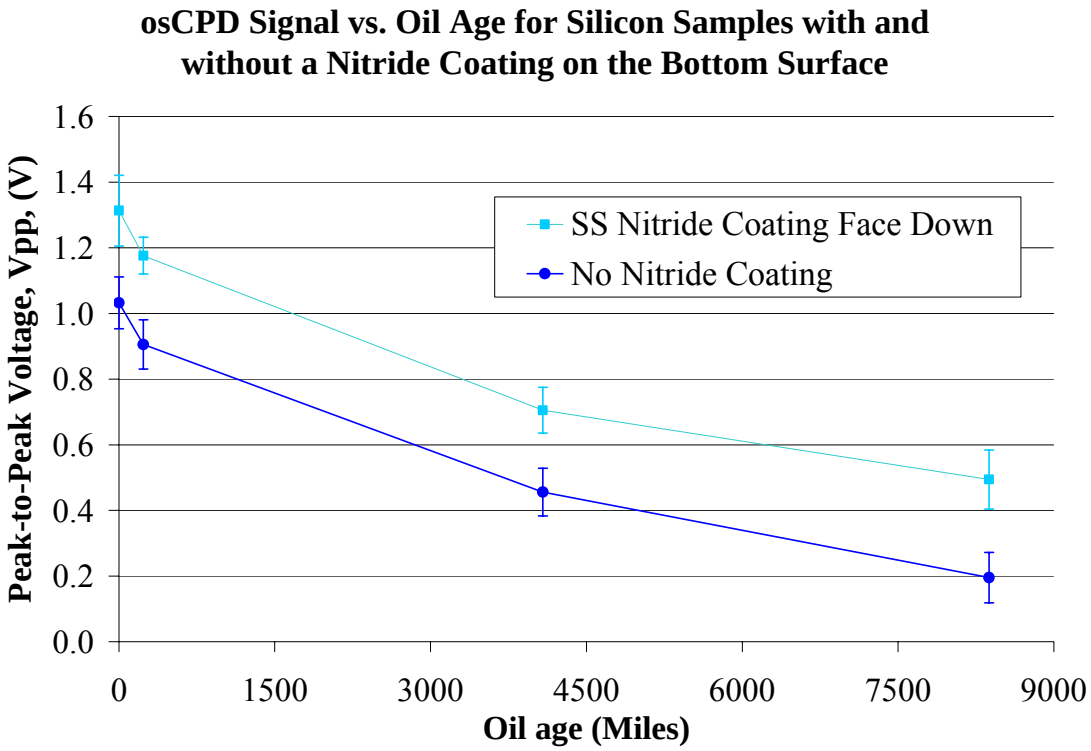

Figure 19. osCPD peak-to-peak voltage (V) versus oil sample age (miles) for two silicon samples: single sided nitride coated silicon sample (oil on non-nitride coated side) and silicon with no nitride coating.

The data in Figure 19 was normalized to point out the similarity of the osCPD response to mileage for the silicon with and without a nitride coating on the underside and no nitride coating where the oil is placed. Normalization was performed by shifting each curve such that the peak-to-peak voltage of new oil was equal to one. The normalized curves for these substrates (Figure 20) reveal that the relation between mileage and osCPD signal is not changed by the addition of the nitride coating.

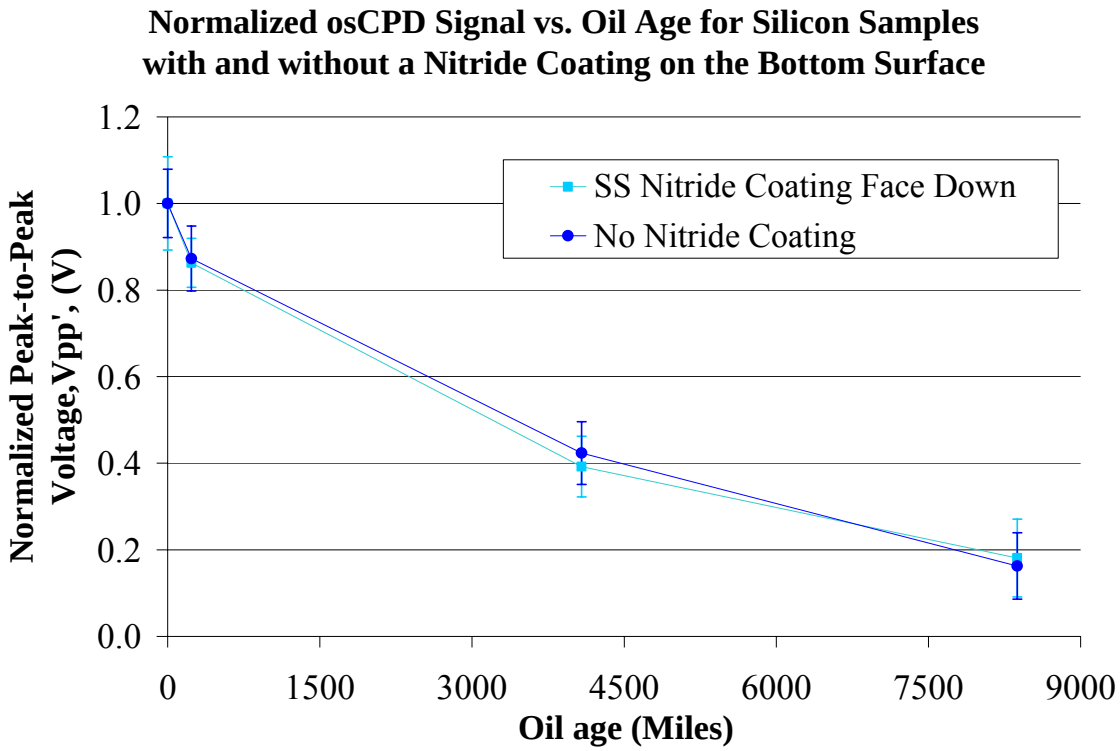

Figure 20. Normalized osCPD peak-to-peak voltage (V) versus oil sample age (miles) for two silicon samples: single sided nitride coated silicon (oil on non-nitride coated side) and silicon without a nitride coating.

Conductivity measurements

Using the process described in the experimental procedure chapter, conductivity measurements were made on the different oil samples. Figure 21 represents the relative conductivity value for oil samples. The relative conductivity value was calculated by dividing each average conductivity measurement by the average conductivity of new oil. The average value was calculated from averaging 1 minute of conductivity measurements, which corresponds to approximately 1000 data points. The error bars represent the 95% confidence interval of this data. The normalized data shows that as mileage increases so does conductivity.

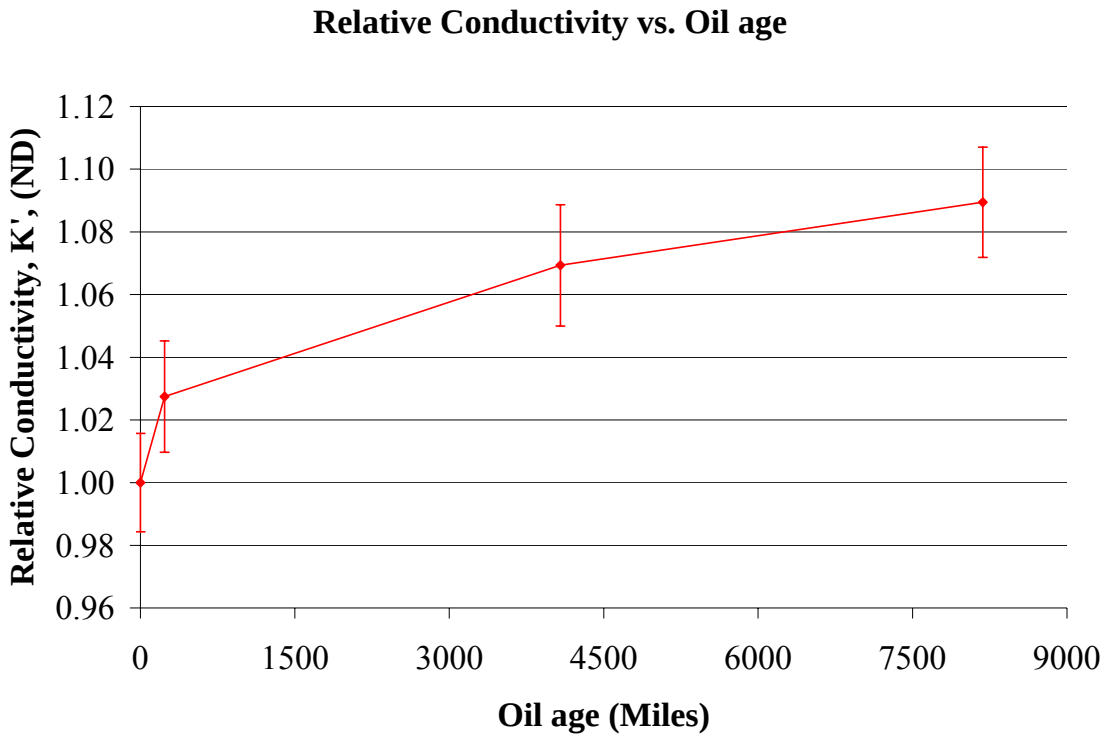

Figure 21. Relative conductivity, which is the conductivity of the oil sample divided by conductivity of new oil (0 miles), versus the oil sample age (miles).

To demonstrate the relation between the osCPD signal and conductivity for increasing mileage, the relative conductivity measurements are plotted (Figure 22) versus the osCPD signal for the aged oil samples from the first oil sample experiment (Figure 16). A linear relationship between these two variables is observed.

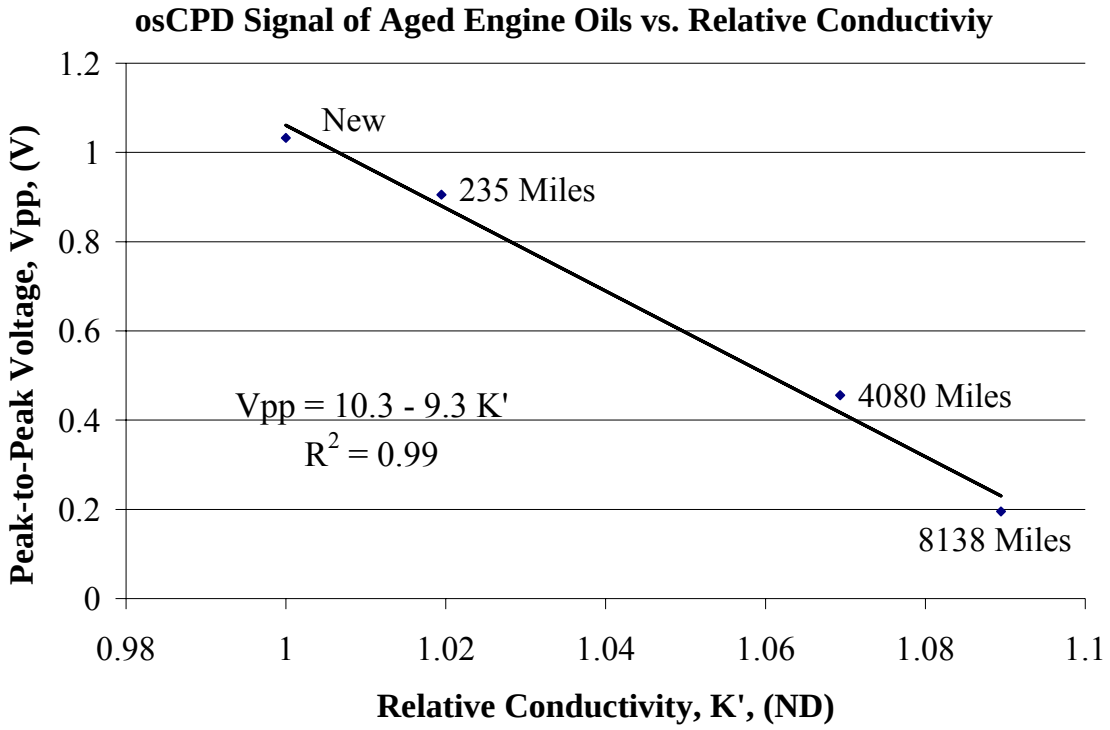

Figure 22. osCPD peak-to-peak voltage (V) of the aged oil samples with the corresponding sample mileage labeled versus relative conductivity, which is the conductivity of the oil sample divided by the conductivity of new oil (0 miles). A linear relationship between peak-to-peak voltage and relative conductivity exists.

CHAPTER 6

DISCUSSION OF RESULTS

This chapter will illustrate the resolution of the osCPD sensor to oil conductivity and relate changes in osCPD due to light properties, mileage and the addition of a nitride layer to the charge transfer process.

Resolution of osCPD sensor to oil properties

The previous results show that there is a linear decrease in the osCPD signal as the conductivity of oil increases (Figure 22). To illustrate the capabilities of the system in monitoring the change in conductivity, the sensors resolution, smallest change in conductivity detectable by the sensor, was determined.

To calculate the resolution, the probes sensitivity to changes in input firsts needs to be known. The sensitivity is defined as the change in peak-to-peak voltage (Vpp) over the change in input (conductivity). The relationship between relative conductivity and Vpp is linear and the sensitivity can readily be defined. From Figure 22, it can be seen that the peak-to-peak voltage changes by 9.28 volts for every unit change in relative conductivity.

The next step in determining resolution is defining the system variance. The largest variance in this set-up is the variance in peak-to-peak voltage between osCPD measurements of an oil sample. As shown in Figure 16, the variances for the different oil samples are consistent. Thus, these variances can be averaged and the resulting system

variation was calculated to be 0.075 volts. With the variance known, the resolution can be calculated as shown below:

$$\text{Resolution} = \frac{\text{Variance}}{\text{Sensitivity}} = \frac{0.075\,\text{V}}{9.28\,\text{V/K'}} = 0.01\,\text{K'} \qquad \textbf{(11)}$$

Therefore, the smallest change in relative conductivity, K', detectable by the osCPD sensor is 0.01.

Effect of Light Intensity on osCPD signal response

The theoretical equation for the peak-to-peak voltage was previously derived in Equation 10 and is restated below:

$$Vpp = G\,(Jph - Js1 - Jbulk - q\,k\,n\,[A]) \qquad \textbf{(12)}$$

As shown in Chapter 5, Figure 13 as the light intensity increases the osCPD signal increases proportionately. This agrees with the developed equation for the signal response. As light intensity increases, Jph, the amount of photoexcited electrons increases and the overall measured osCPD signal increases proportionately.

Effect of Mileage on osCPD signal response

The parameters of Equation 12 are assumed to be constant except for, [A], the concentration of acceptor species at the surface. This assumption is made because the oil film on the silicon surface is the only parameter varying between experiments. The results support this assumption as repeat measurements of the same oil provide consistent results.

The overall equation for the voltage developed in the osCPD probe, restated in Equation 12, can be simplified by substituting in Equation 13 and 14 for the constant terms:

$$Jc = Jph - (Js1 + Jbulk) \quad \textbf{(13)}$$

$$N = q\ k\ n \quad \textbf{(14)}$$

After performing this substitution, the resulting osCPD signal is:

$$Vpp = G\ (Jc - N\ [A]) \quad \textbf{(15)}$$

Thus the osCPD signal is linearly related to the concentration of acceptor species. This concentration seems to be linearly related to the conductivity of the oil. The conductivity is a measure of impurities in the oil.[17-18] Thus by increasing the impurities, it is thought that the number of sites where electrons recombine also increases. Therefore the concentration of acceptor species, [A], can be replaced by the conductivity, K, resulting in following osCPD equation:

$$Vpp = Jc - N*K \quad \textbf{(16)}$$

The experimental results agree with this relationship. There is a proportional decrease in osCPD signal with increasing oil mileage and this signal is linearly related to conductivity as shown previously in Figure 22. The linear relation found between the measured osCPD signal and relative conductivity was:

$$Vpp \approx 10\ (1 - K') \quad \textbf{(17)}$$

which agrees with the form of Equation 16.

Effect of Nitride Coating on osCPD response

To further demonstrate that the changes in osCPD signal are caused by a charge transfer process, the nitride coating experiments were performed. The osCPD response to oil properties was evaluated on the substrates (12a through 12d) shown previously in Figure 12. The signal dependence on oil age was the same for 12a and 12b silicon (no nitride between oil and silicon interface). Experiments using these substrates both showed a decrease in signal with increasing mileage (Figure 19), but the sample 12b (nitride film on bottom) had proportionately larger values. For the other two samples, 12c and 12d where the nitride layer was between the oil and silicon interface, the osCPD signal did not change with oil age (Figure 17). But like the previous two samples, the substrate with the nitride coating on the bottom (12d) had a larger value.

For samples 12c and 12d, placing a nitride layer on surface 2 of the silicon sample (where oil is placed) removed the signal dependence on oil mileage. For this experiment, the equation for the osCPD response is again:

$$Vpp = G\,(Jph - Js1 - Jbulk - Js2) \qquad \textbf{(18)}$$

where the recombination at surface 2, Js2, is defined by the oil and nitride interface, not the oil and silicon interface. Thus the Js2 recombination will not change with oil properties because the charge interaction is with the fixed nitride layer. Since the remainder of the terms in Equation 18 are constant, then there should be no changes in osCPD signal when different oils are placed on the nitride coated substrate. The results agree with this explanation. Figure 17 for the single and double sided nitride coated film (oil on nitride coated side) verify that there is no significant change in signal with oil age. This supports that the change in signal is due to charge interaction at the silicon and oil

interface, since adding a layer to separate these layers removed the signal dependence on age.

The results also showed that adding a nitride layer to the bottom surface increased the osCPD signal magnitude (Figure 17 and Figure 19). This can be explained since the nitride coating on the underside of the silicon acts as an antireflective coating.[19] This coating allows more light into the substrate. This increase boosts the amount of photo-excited electrons created in the silicon and therefore increases the photocurrent, Jph. As the photocurrent increases, it can be seen from Equation 18 that the total measured signal is also greater. Thus the model agrees with the experimental results, as more light enters into the substrate the signal increases. Plus it shows that increasing the amount of light into the system does not alter the trend between oil properties and osCPD signal.

CHAPTER 7

CONCLUSIONS

This research shows that the novel optically stimulated Contact Potential Difference sensor can be used to monitor oil conductivity as engine mileage increases, and that the change in signal is attributed to a surface charge interaction at the silicon and oil interface. The following conclusions were drawn from this thesis.

1. The osCPD peak-to-peak voltage decreases as the mileage of the engine oil sample increases.
2. The osCPD peak-to-peak voltage (Vpp) is linearly related to the relative conductivity, K', of the engine oil sample as described by:

$$Vpp \approx 10\,(1 - K') \qquad \textbf{(19)}$$

   The relative conductivity was defined as the conductivity of the oil sample divided by the conductivity of new oil.
3. The sensor can detect a 0.01 change in relative conductivity.
4. The addition of a nitride layer between the oil and silicon interface eliminates the change in osCPD signal due to mileage or conductivity.

CHAPTER 8

RECOMMENDATIONS

To further improve this system, the following recommendations are made:

1. Investigate alternate measurement techniques that would eliminate the need to clean the silicon substrate in between measurements. The cleaning process currently hinders the ability of the system to perform online measurements of oil properties.
2. Replace light source with light emitting diodes to help miniaturize the system for on-line oil monitoring.
3. Investigate alternate uses of the osCPD sensor in monitoring charge transfer interactions.

APPENDIX A

MOTION CONTROL SOFTWARE

Motion Control Software User Interface

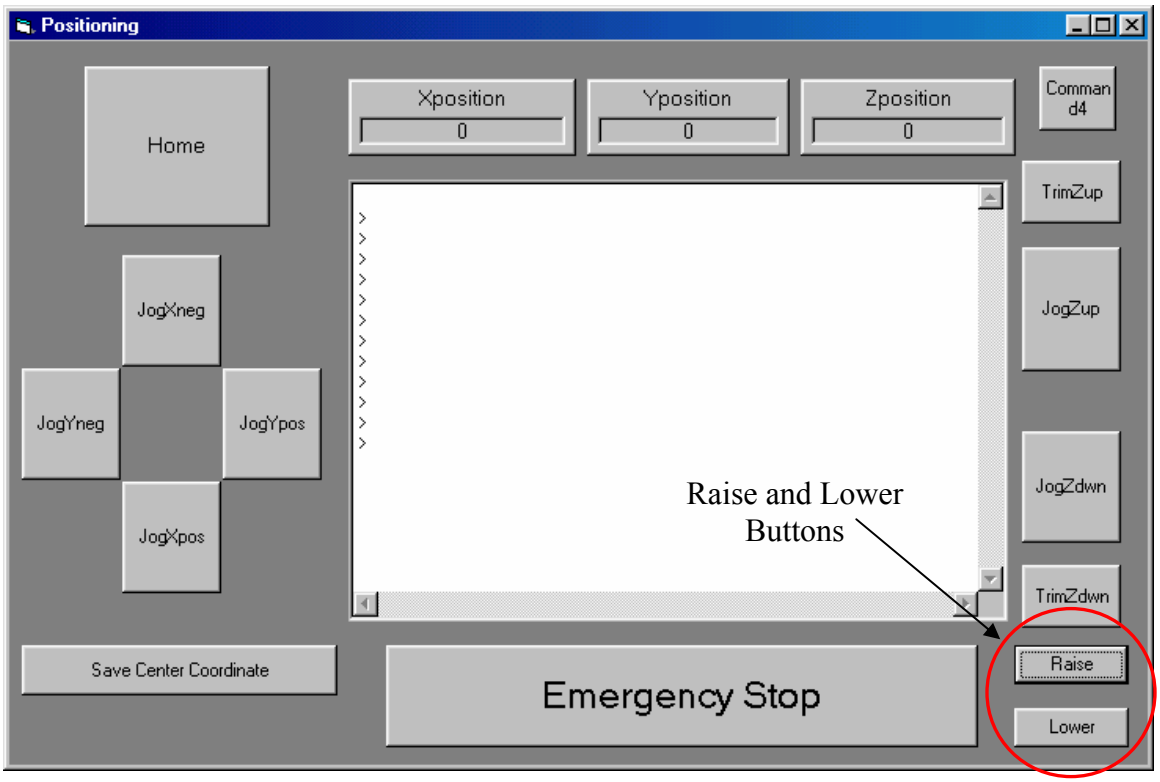

Figure 23. Motion control software user interface with raise and lower buttons labeled.

Code for Motion Control Software

```
// Command for Lowering the probe.
Private Sub Lower()
   chars_sent = Comm60001.SendCommand("MA111")
   chars_sent = Comm60001.SendCommand("MA111")
   chars_sent = Comm60001.SendCommand("d0,0,6200")
   chars_sent = Comm60001.SendCommand("go0,0,1")
End Sub

// Command for Raising the probe.
```

```
Private Sub Raise()
   chars_sent = Comm60001.SendCommand("MA111")
   chars_sent = Comm60001.SendCommand("MA111")
   chars_sent = Comm60001.SendCommand("d0,0,0")
   chars_sent = Comm60001.SendCommand("go1,1,1")
End Sub
```

APPENDIX B

USER INTERFACE FOR DATA AQUISTION SYSTEM

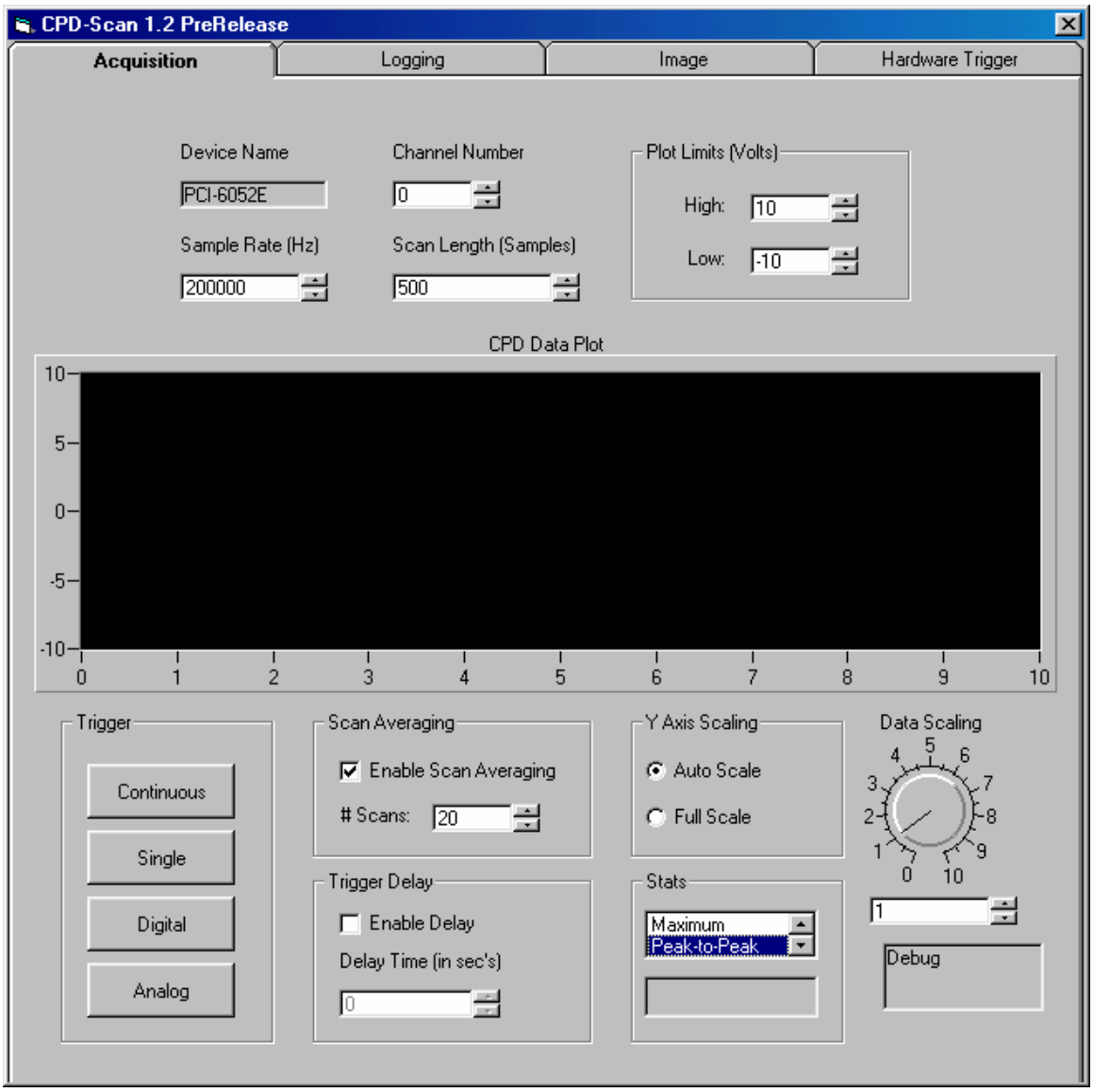

Figure 24. CPD-Scan data acquisition user interface.

APPENDIX C

USER INTERFACE FOR QUAD SOFTWARE

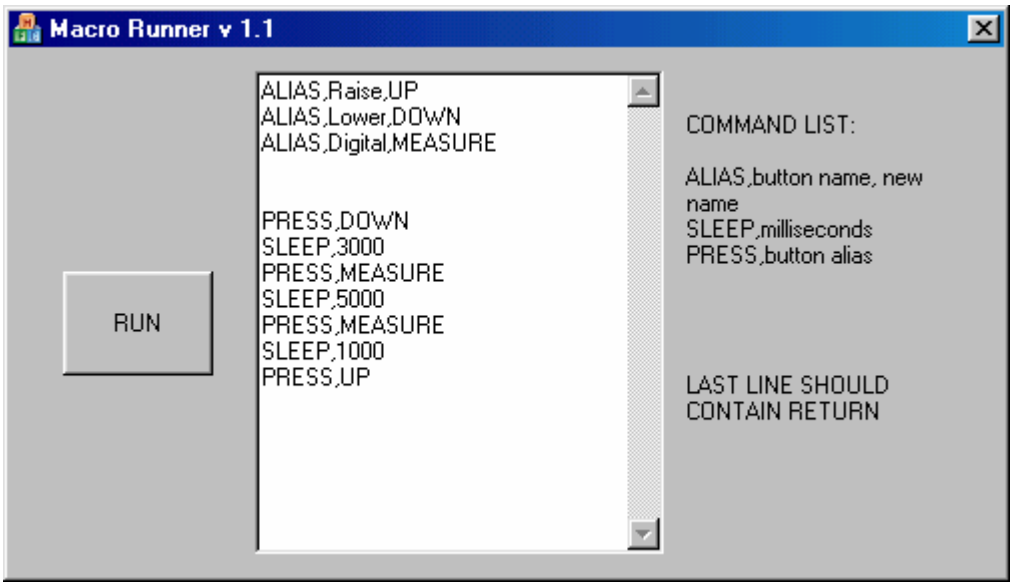

Figure 25. Quad software interface with code entered to control other software.

APPENDIX D

RANDOMIZATION ORDER

Table 4. Randomization Order for Oil Sample Experiment 1.

Experimental Order	Sample Type
1	No Oil
2	235
3	No Oil
4	4080
5	No Oil
6	8138
7	No Oil
8	New
9	No Oil
10	235
11	No Oil
12	4080
13	No Oil
14	8138
15	No Oil
16	235
17	8138
18	No Oil
19	4080
20	New
21	No Oil
22	8138
23	New
24	235
25	No Oil
26	New
27	No Oil
28	8138
29	No Oil
30	4080
31	No Oil

Table 4 (continued).

Experimental Order	Sample Type
33	No Oil
34	8138
35	No Oil
36	235
37	No Oil
38	4080

Table 5. Randomization Order for Oil Sample Experiment 2.

Experimental Order	Sample Type
39	No Oil
40	8138
41	No Oil
42	235
43	No Oil
44	4080
45	4080
46	None
47	8138
48	None
49	New
50	None
51	4080
52	None
53	235
54	None
55	New
56	None
57	8138
58	None
59	4080
60	235
61	4080
62	8138
63	New
64	235

Table 5 (continued)

65	New
66	235
67	New

APPENDIX E

SUMMARY OF STATISTICAL ANALYSIS PERFORMED ON EXPERIMENTAL RESULTS

The 2 sample t-test, with significance level 95%, was used to analyze whether the means illustrated in Table 6 were significantly different. This test evaluates whether the mean between two samples is the same or different as shown in hypothesis below:

Hypothesis:

Ho: $\mu 1 - \mu 2 = 0$

Ha: $\mu 1 - \mu 2 \neq 0$

Table 6. Summary of statistical results for 2-sample t-tests performed on data from different experimental tests.

Experiment Description	μ1 Oil Sample	μ2 Oil Sample	p-value	Significant difference between sample means?
Oil Sample Experiment 1 (osCPD Vpp)	No Oil	0 miles	0.873	No
	0 miles	235 miles	0.004	Yes
	235 miles	4080 miles	0.000	Yes
	4080 miles	8376 miles	0.001	Yes
Conductivity tests (Relative conductivity)	0 miles on DSN	8376 on DSN	0.300	No
	0 miles on SS Nitride Up	8376 on SS Nitride Up	0.096	No

REFERENCES

[1] N. Ashcroft and N. Mermin, *Solid State Physics*. Holt: New York, 1976.

[2] L. Kelvin, G. Fitzgerald, and W. Francis, "Contact Electricity of Metals." *Philosophical* Magazine and Journal of Science, (1898): 80-120.

[3] W. A. Zisman, "A New Method of Measuring Contact Potential difference in Metals." *Scientific Instruments,* 3, (1967): 367-370.

[4] E. Zanoria, K. Hamall, S. Danyluk, and A.L. Zharin, "The Non-vibrating Kelvin Probe and its Application for Monitoring Surface Wear." *Journal of Testing and Evaluation*, 25, (1997): 233-238.

[5] A. Fahrenbruch, and R. H. Bube, *Fundamentals of Solar Cells: Photovoltaic Solar Energy Conversion*. Academic: New York, 1983.

[6] R. Memming, *Semiconductor Electrochemistry*. Wiley: New York, 2001.

[7] A. Juang, "Effects of Surface Modification on Charge-Carrier Dynamics at Semiconductor Interfaces." *PhD Thesis*, California Institute of Technology, 2002.

[8] J. Schmidt, and A. Aberle, "Carrier recombination at silicon-silicon nitride interfaces fabricated by plasma-enhanced chemical vapor deposition." *Journal of Applied Physics*, 85, (1999): 3626-3633.

[9] M. Kerr, and Cuevas, "Recombination at the interface between silicon and stoichiometric plasma silicon nitride." *Journal of Applied Physics*, 17, (2002): 166-172.

[10] D. Yano, C. Korach, J.Streator, and S. Danyluk, "Nonvibrating Contact Potential Difference Probe Measurement of a Nanometer-Scale Lubricant on a Hard Disk." *Transactions of the ASME*, 121, (1999): 980-983.

[11] A. Watt, "Fringer field corrections in nvCPD applications," *Masters Thesis*, Georgia Institute of Technology, (To be published).

[12] Amptec Inc, "A250F/N Charge Sensitive Preamplifer Data Sheet."

[13] D. Levermore, M. Josowicz, W. Rees Jr, and J. Janata, "Headsapce Analysis of Engine Oil by Gas Chromatography/Mass Spectrometry." *Analytical Chemistry*, 73, (2001): 1361-1365.

[14] K. Sepic, M. Josowicz and J. Janata, "Determination of the principal volatile compounds in degraded engine oil." *Tribology and Lubrication Technology*, (2004): 48-55.

[15] K. Hermansson, U. Lindberg, B. Hok, and G. Palmskog, "Wetting properties of Silicon." *Transducers*, (1991): 193-196.

[16] Schott Fostec Inc, "Ace 50W Light Source Data Sheet," (2001).

[17] C. Megerle, "Oil quality monitor sensor and system." US Patent 5089780, (1992).

[18] R. Kauffman, "On-Line and Off-Line Techniques for Monitoring the Thermal and Oxidative Degradations of Aircraft Turbine Engine Oils-Part 1: Laboratory Experiments." *ASME/STLE Tribology Conference*, (1994) 1-7.

[19] W. Sexton, "Plasma Nitride AR Coatings for Silicon Solar Cell." Solar Energy Mater, 7, (1982): 1-14.